Tissue Polarity Genes of *Drosophila* Regulate the Subcellular Location for Prehair Initiation in Pupal Wing Cells

Lily L. Wong and Paul N. Adler

Biology Department, Molecular Biology Institute, and Cancer Center, University of Virginia, Charlottesville, Virginia 22901

Abstract. The *Drosophila* wing is decorated with a regular array of distally pointing hairs. In the pupal wing, the hairs are formed from micro-villus like prehairs that contain large bundles of actin filaments. The distal orientation of the actin bundles reveals the proximal-distal polarity within the pupal wing epithelium. We have used F-actin staining to examine early stages of prehair development in both wild-type and mutant pupal wings. We have found a striking correlation between hair polarity and the subcellular location for assembly of the prehair. In a wild-type wing, all of the distally pointing hairs are derived from prehairs that are formed at the distal vertex of the hexagonally shaped pupal wing cells. Mutations in six tissue polarity genes result in abnormal hair polarity on the adult wing, and all also alter the subcellular location for prehair initiation. Based on their cellular phenotypes, we can place these six genes into three phenotypic groups. Double mutant analysis indicates that these phenotypic groups correspond to epistasis groups. This suggests that the tissue polarity genes function in or on a pathway that controls hair polarity by regulating the subcellular location for prehair formation.

TISSUE and cell polarity is found in all multicellular organisms. The most common form is the apical–basal polarity found in epithelial cells. In this paper, we are concerned with polarity within the plane of an epithelium, and the possible role of coordinating the cytoskeletons of individual cells for tissue level morphogenesis (Tucker, 1981).

The cuticular landscape of *Drosophila* contains large numbers of sensory bristles and hairs (cellular projections). For example, posteriorly pointing bristles and hairs are found on the notum and abdomen, and distally pointing hairs are found on the wings. The common orientation of these structures gives rise to what we call "tissue polarity" (i.e., polarity within the plane of an epithelial tissue surface (Vinson and Adler, 1987; Adler, 1992)). For several reasons we have chosen the *Drosophila* (pupal and adult) wing as a model system for studying the morphogenesis of tissue polarity. The wing is a relatively homogeneous and simple tissue. Almost every cell in the pupal wing elaborates a single distally pointing prehair that becomes the cuticular adult hair. Thus, possible complications arising from cell type–specific differentiation are not present. At the time the prehairs develop, all cell division has ceased on the pupal wing (Garcia-Bellido and Merriam, 1971; Schubiger and Palka, 1987), thus there are no complications arising from cell division. Further evidence for the independence of tissue polarity from growth comes from the observations of Gubb and Garcia-Bellido (1982), who found that changes in wing size did not affect either wild-type or mutant tissue polarity patterns. Finally, the pupal wing is structurally quite simple, consisting of a one-cell layer thick epithelium folded on itself. The adult wing, which displays the regular array of distally pointing hairs, consists primarily of nonliving cuticle produced by the pupal wing cells. The flatness of both the pupal and adult wings provides substantial advantages for observation of whole-mount preparations. Thus, this simple tissue is an excellent model system for both genetic and cell biological approaches to the study of tissue polarity.

We stained pupal wings with fluorescently conjugated phalloidin (which binds specifically to F-actin, Wulf et al., 1979) and observed strong staining within the early prehairs. We then used F-actin staining to analyze the early events of prehair development in wild-type and mutant pupal wings. In wild-type wings, we found that a prehair formed at the distal vertex of each hexagonally shaped pupal wing cell. From its earliest appearance, a prehair had a distal polarity, arguing that hair polarity is regulated at the level of initiation of prehair formation. The pupal prehair pattern was reminiscent of the adult cuticular hair pattern.

Mutations in tissue polarity genes result in the formation of adult cuticle with abnormal tissue polarity patterns (Gubb and Garcia-Bellido, 1982; Held et al., 1986). To a first approximation, the structure of an individual hair or bristle sense organ is normal. What the mutants alter is the orientation of these structures with respect to the body as a whole (e.g., wing hairs not pointing distally). We examined the adult wing hair patterns, and the location of prehair formation in pupal wings carrying mutations in the *frizzled* (*fz*), *disheveled* (*dsh*), *prickle* (*pk*), *inturned* (*in*), *fuzzy* (*fy*), and *multiple-wing-hair* (*mwh*) tissue polarity genes (Gubb and Garcia-Bellido, 1982; Held et al., 1986; Adler et al., 1987).

Although we restricted our analyses to the wing, these mutations cause polarity disruption in other body regions as well (Gubb and Garcia-Bellido, 1982; Held et al., 1986). In this paper, we show that in the pupal wing, all of the tissue polarity mutations resulted in an abnormal subcellular location for the formation of the prehair. This striking correlation between hair polarity and the subcellular location for prehair formation suggests that hair polarity is controlled by regulating the subcellular site for prehair formation and that the tissue polarity genes regulate the choice of this site within the cell.

We were able to place the six genes into three groups based on their cellular phenotypes in the wing (i.e., prehair initiation site and the average number of hairs per cell). The first group consisted of *fz*, *dsh*, and *pk*, the second of *in* and *fy*, and the third of *mwh*. We examined both adult and pupal wings of all of the double mutant combinations. We found that the group 2 and 3 mutations are epistatic to the group 1 mutations, and the group 3 mutation is epistatic to the group 2 mutations with respect to the cellular phenotypes. Based on these results, we suggest that the tissue polarity genes form a regulatory pathway, with the group 2 and 3 genes downstream of the group 1 genes.

Materials and Methods

Drosophila Strains and Mutants

Fly stocks were maintained at 24.5 ± 0.5°C. Oregon-R flies were used as the wild type. All the mutations are described in Lindsley and Zimm (1992). The *fz* alleles used in this study are also described in detail in Adler et al. (1987, 1990). We used fz^{1} and fz^{CT8CX2}/fz^{KD4a} for single and double mutant analyses. Both genotypes show a strong (null or near null) phenotype, and fz^{CT8CX2}/fz^{KD4a} is a protein null genotype (Liu, J. and P. N. Adler, unpublished observation). We also examined weak (*R53*), moderate (*G11a*), and cell autonomous (*N21*) *fz* alleles in this study. The *pk* and *spiny legs* (*sple*) genes are located very close to each other on the second chromosome, and are likely to represent a single complex locus (Gubb and Garcia-Bellido, 1982; Gubb, D., personal communication). In this paper, we will consider *pk/sple* as a single locus, and abbreviate the locus as *pk*. The pk^{1} allele used in this study appears to be a phenotypic null allele (Gubb and Garcia-Bellido, 1982). *dsh* is the only one of these genes that is essential for viability. Mutations in *dsh* zygotically cause late larval lethality. Embryos that also lack the *dsh* maternal contribution die and have a segment polarity mutant phenotype (Perrimon et al., 1987). The allele used in this study (dsh^{1}) is adult viable and fertile, and complements the larval lethality of other alleles (Perrimon et al., 1987). Mitotic clones of lethal alleles in adult cuticle show a phenotype that is similar to the adult viable allele (Klingensmith, J., and N. Perrimon, personal communication). We used in^{1} in this study, which is phenotypically close to a null mutation (Gubb and Garcia-Bellido, 1982; P. N. Adler, unpublished observation). The fy^{2} allele used in this study is phenotypically close to a null allele (Jones, K., and P. N. Adler, unpublished observation). The mwh^{1} allele used in this study shares a similar phenotype with another *mwh* allele recently isolated in this laboratory.

Double mutants were constructed and maintained using *FM7*, an X chromosome balancer; *CyO*, a second chromosome balancer; or *TM3*, or *TM6B*, both of which are third chromosome balancers. These balancers are described in Lindsley and Zimm (1992).

Adult Wings Preparation

Adult wings from wild-type and homozygous mutants were dehydrated in ethanol and mounted in euparal as described in Adler et al. (1987).

Analysis of Adult Wing Phenotypes

Wing Hair Patterns. The dorsal surface of at least 10 wings was examined for each genotype. For mutations in all of the genes studied, the hair polarity pattern on the ventral surface is more abnormal than that on the dorsal surface. We used the dorsal surface in our studies because the dorsal hairs are larger, darker, and easier to examine. Our less extensive observations on the ventral surface lead us to the same general conclusions as for the dorsal surface. We attempted to devise a scheme to describe the complex mutant hair polarity patterns on the wing that simplified the data but retained salient features of the patterns. An adult wing is divided into regions A–E that are demarcated by wing veins (see also Fig. 3 *a*). We considered the polarity of each region separately and schematically used five equally sized stripes to represent the five regions (see Fig. 5). We subdivided each region into 5 or 8 equal-length parts along the proximal–distal axis. For any subdivision where 60% or more of the hairs had a common polarity, the subdivision was assigned that polarity. As a further simplification, we used eight orientations that differed by 45° to approximate the orientation of the hairs in any subdivision. As shown in Fig. 5, these subdivisions have arrows showing their approximate orientation. Blank subregions have hairs with a distal polarity (that is, a wild-type polarity). We call any region where neighboring hairs share a common abnormal (i.e., not distal) polarity abnormal patches (APs).[1] In some subdivisions, there was not a particular polarity shared by 60% or more of the hairs, and these were filled in grey in Fig. 5. This could be due to one of two different reasons. In some subdivisions, there were places where the hairs of neighboring cells were not aligned, we call such locations abnormal foci (AFs). The *fz* wings in Figs. 4 *e* and 7 *f* show examples of small AFs. In other subdivisions filled in grey, there were regions where most hairs were aligned with their neighbors (as we described for AP), but where no particular orientation was common among >60% of the cells. This was because the subdivisions contained several regions of different APs. Part of such a region can be seen in the *dsh; pk* wing in Fig. 4 *q*.

The Average Number of Hairs per Cell. To assess the average number of hairs per cell for each genotype, we counted 100 cells on the dorsal surface in the C region immediately anterior to the posterior cross-vein in region D. The region scored formed a rectangle ~5 cells wide and 20 cells long along the distal proximal axis. This relatively central region is strongly affected by mutations in all of the tissue polarity genes, and has been used in other studies carried out in this laboratory. In a number of experiments, other regions of the wing have been similarly scored. While quantitative differences are seen in the fraction of multiple hair cells in different regions of the wing, the same qualitative conclusions are reached regarding the strength of individual alleles and phenotypes of group 1, 2, and 3 mutations. The numbers represent the mean value from scoring five wings.

Fluorescent Phalloidin Staining of Pupal Wings

White prepupae (0 h) were collected and typically transferred to an 18 ± 0.5°C incubator. Pupae were dissected between 68 and 74 h to study the different stages of prehair development. In some experiments, the pupae were incubated at 25°C. All surgical and staining manipulations were carried out at room temperature (RT). Pupae were adhered to a piece of double-sided tape attached to a microscope slide. They were dissected from their pupal cases, immersed in 8% *p*-formaldehyde in 0.1 M phosphate buffer, pH 7.2, and the pupal wings were removed. The pupal wing was removed from its cuticular sac, and fixed for an additional 10 min. The overall fixation time was ~20 min. The wings were rinsed 1×, 5 min, and then 2×, 10 min each, with PBS (0.13 M NaCl, 0.01 M phosphate buffer, pH 7.0), followed by staining with rhodamine-phalloidin or fluorescein-phalloidin (0.33 μM, 350 μl, Molecular Probes, Inc., Eugene, OR) in PBS in a light-proof moist chamber for 30 min. The wings were washed as before, and mounted in 1:9 PBS:glycerol mountant that contained 1 mg/ml of *p*-phenylenediamine (Sigma Chemical Co., St. Louis, MO). Wings were viewed under EPI fluorescence using a Zeiss Axiophot microscope with a Planneofluar 100×/1.30 objective (Carl Zeiss, Inc., Thornwood, NY). Micrographs were taken using either Tri-X Pan or T-MAX-400 films (Eastman Kodak Co., Rochester, NY). Data were collected from at least six pupal wings for each genotype. For most of the genotypes, >15 wings were examined.

In control experiments, Ore-R pupal wings were prepared as before, but then preincubated for 20 min in a buffer containing 10× unlabeled phalloidin (3.3 μM). These wings were then stained for 30 min in the presence of both labeled and unlabeled phalloidin (rhodamine-phalloidin, 0.33 μM; unlabeled phalloidin, 3.3 μM; final concentrations). Wings were washed, mounted, and examined as before. Such control wings were then compared

1. *Abbreviations used in this paper*: AF, abnormal focus; AP, abnormal patch; RT, room temperature.

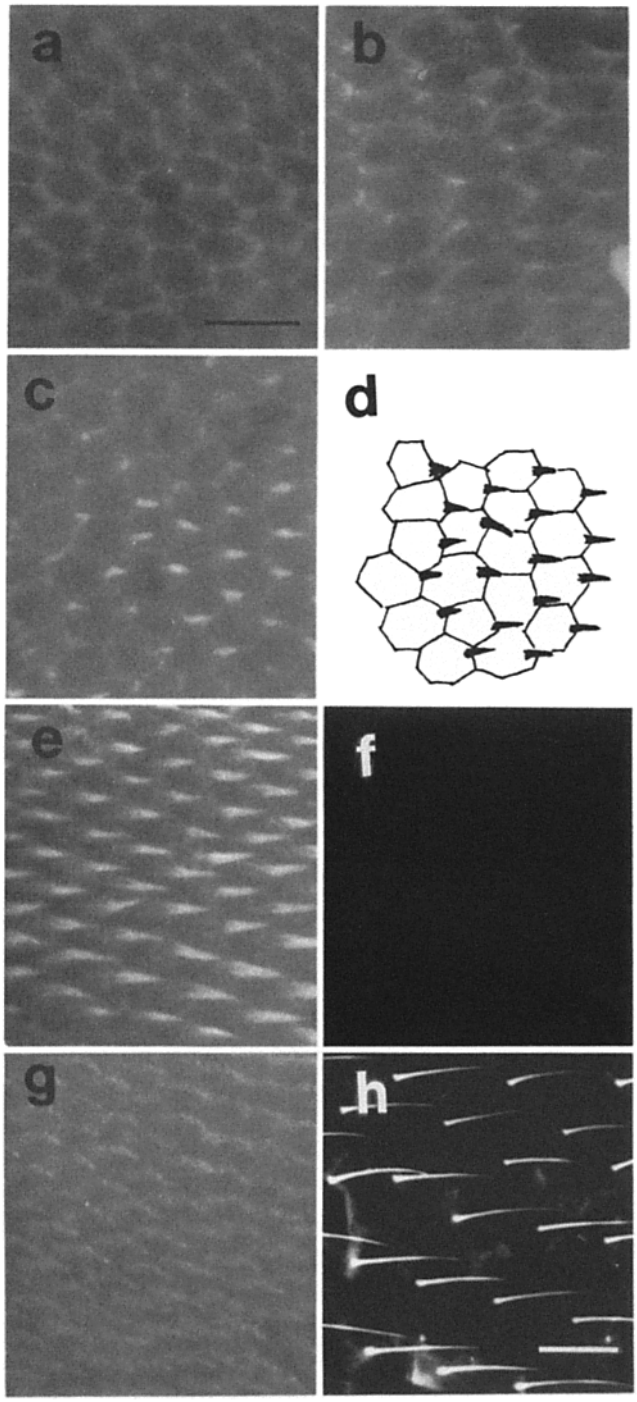

Figure 1. Wild-type prehair development of *Drosophila melanogaster* examined by rhodamine–phalloidin staining. Orientation for all the light micrograph figures is as follows: proximal, left; distal, right; anterior, top; posterior, bottom. See also Fig. 3 *a* for a drawing of a pupal wing. Individual light micrographs are not from the same region of the pupal wing. (*a*) Pupal wing cells before prehair differentiation. F-actin bundles were found outlining the hexagonally shaped cells near the apical region of the epithelium, with brighter staining at cell vertices. (*b*) At the onset of prehair differentiation, increased F-actin staining was observed at the distal vertex of each cell. (*c*) Elongating prehairs filled with F-actin pointed distally and appeared to lie flat on their distal neighbors. (*d*) An interpretive drawing of *c*; note the hexagonally shaped cells, and the distally pointing prehairs initiated from the distal vertex of individual cells. (*e*) A panel to show a pupal wing at a later stage of prehair differentiation and as a control for the competition experiment to demonstrate the specific staining by rhodamine–phalloidin. The prehairs were brightly stained suggesting that they were filled with F-actin bundles. They seemed to have extended deeper into the cells. Prehairs had elevated above the epithelium (pupal wing surface), therefore the cell periphery staining was less prominent due to being out of the plane of focus. (*f*) An experimental pupal wing preincubated with 10× unlabeled phalloidin (see also Materials and Methods). We did not observe any nonspecific staining of rhodamine–phalloidin in these treated wings. This shows that the binding of rhodamine–phalloidin to the F-actin within the prehairs is very specific. *e* and *f* were processed in the same manner with respect to every photographic manipulation. (*g*) A pupal wing stained with an anti-actin mAb to confirm that actin molecules are present in the prehairs. This antibody stained the prehairs, but the staining was not as bright as by rhodamine–phalloidin. (*h*) A scanning electron micrograph of an adult wing from a small mid C region. The cuticular hairs were the remnants of the once F-actin–filled prehairs. These hairs were evenly spaced and had retained their distal polarity. All the scanning electron micrographs were taken from the same region of the adult wing on the dorsal surface. Bars: (*a–g*) 10 μm, (*h*) 15 μm.

to wings simultaneously stained via our standard procedure. The same experiment was performed with 33 μM unlabeled phalloidin (100× more concentrated than labeled phalloidin). Micrographs from control and experimental pupal wings were taken and processed under the same conditions. Films were exposed for 3.36 s. Prints were exposed for 15 s and developed for 2 min on Kodak F3 papers.

Antibody Staining

Ore-R pupal wings were fixed as before. Half of the wings were treated following the standard rhodamine–phalloidin staining procedure. We followed the procedure of Bopp et al. (1991) for the anti-actin staining. Briefly, wings to be treated with antibody were rinsed 3×, 20 min each with a detergent mix (0.5% Triton-X, 0.05% NP-40, 0.5% Tween-20 [Sigma Chemical Co.], in PBS, pH 7.0) with 4% milk powder. All steps were carried out at RT. These wings were then incubated with an anti-actin mouse mAb (Amersham Corp., Arlington Heights, IL), 1:500 in 0.1% Triton-X/PBS for 1 h. Wings were washed 3×, 10 min each with PBS containing 0.1% Triton-X and 2% BSA (Sigma Chemical Co.). They were then incubated with a goat anti-mouse fluorescein-conjugated antibody (Molecular Probes, Inc.), 1:200 in the same wash buffer for 1 h in a light-proof moist chamber. After rinsing 3×, 10 min each with 0.1% Triton-X/PBS, they were mounted and examined as before. Two alternative antibody staining procedures were also used. These differed in the approach for permeabilization of the wing tissue and in the blocking agents. Similar results were obtained by all three procedures.

Scanning EM Specimen Preparation

Right wings were removed from anesthetized adult flies. Three wings of the same genotype, dorsal side up, were adhered to a scanning EM stub via a dab of low resistance contact cement (Ernest F. Fullam, Inc., Latham, NY). They were examined in an Autoscan (ETEC Corporation, Hayward, CA) scanning electron microscope shortly after preparation.

Electron Microscopy Specimen Preparation

Pupal wings were dissected as before but were fixed in Karnovsky fixative (1.0% glutaraldehyde, 1.0% *p*-formaldehyde in 0.1 M phosphate buffer, pH 7.2) for 2 h at RT. The subsequent steps were carried out on ice. The wings were washed 2×, 15 min each with 3.5% sucrose in the same phosphate buffer, followed by postfixation in 2% osmium tetraoxide in 0.1 M phosphate buffer. They were dehydrated in ethanol and transferred to propylene oxide at RT. Individual wings were embedded in Epon 812, and were sectioned on a Sorvall Porter-Blum MT-2 ultra-microtome. 600–800-Å-thick sections were stained with 4% uranyl acetate for 10 min, followed by lead citrate for 5 min. Longitudinal sections were examined at 60 kV with a Philips EM 200 electron microscope (Philips Technologies, Cheshire, CT).

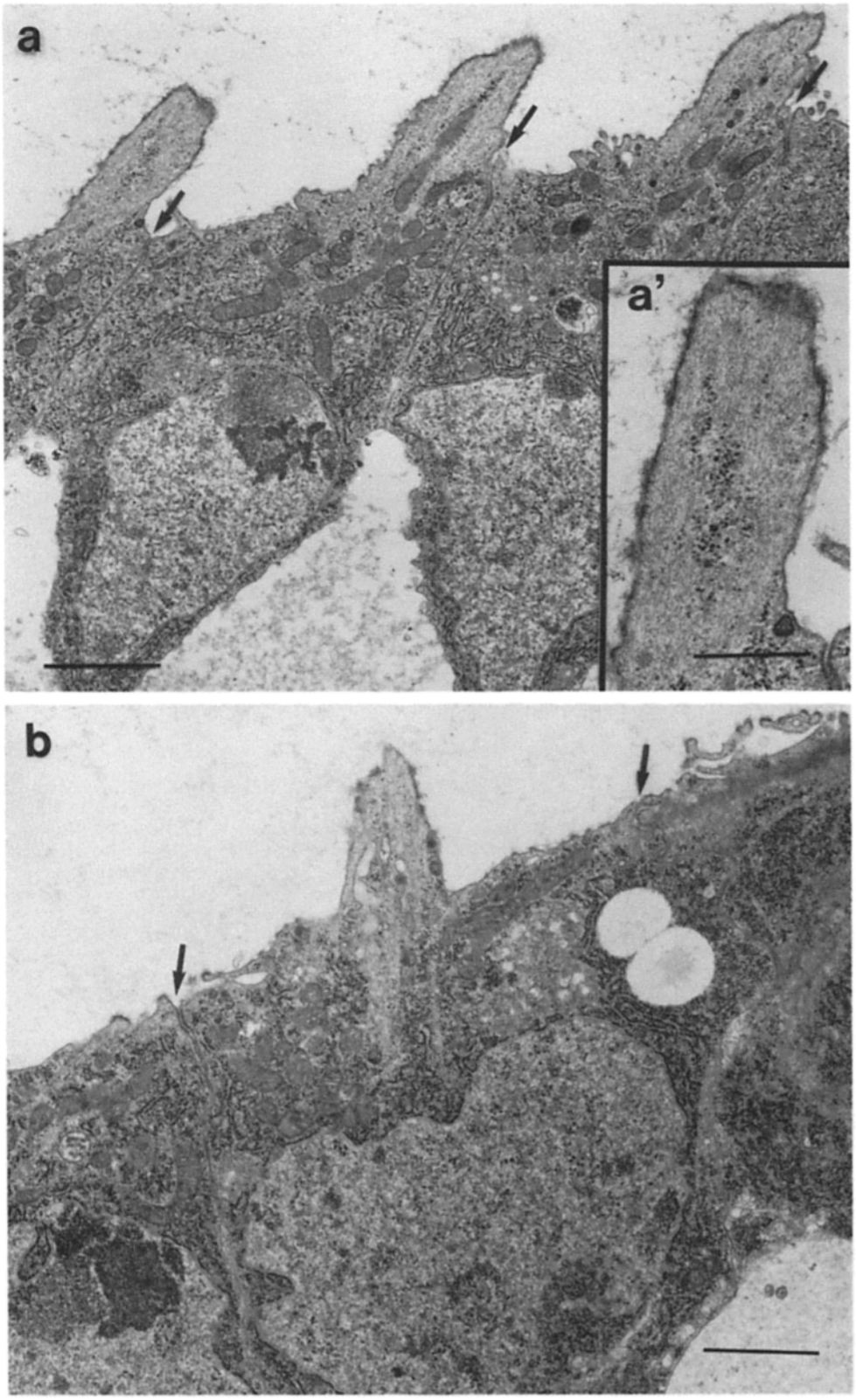

Figure 2. Electron micrographs of longitudinal sections of wild type and *fz* mutant pupal wings. Orientation is the same as in Fig. 1. Arrows point to the cell boundaries. (*a*) Section of a wild-type pupal wing near the distal region where prehairs had elevated from the wing surface. Each wild-type prehair initiated from the distal most edge of a cell and pointed distally. (*a'*) A high magnification of a prehair showing the fiber-like material (probably F-actin) inside. Note that the fibers did not fill the prehairs completely. (*b*) Section of a *fz* mutant pupal wing at a similar developmental stage as in *a*. Note that the prehair did not initiate from the distal edge of the cell. Apart from the prehair initiation site and orientation, the cellular morphology of this pupal wing cell was identical to a wild-type cell. Bars: (*a* and *b*) 1.63 μm; (*a'*) 0.65 μm.

Results

Wild-type Wing Hair Development

In our initial experiments, we found that prehairs stained very brightly with rhodamine–phalloidin (Fig. 1 *e*), suggesting the presence of large bundles of actin filaments in the prehairs. This staining was eliminated when the tissue was preincubated in unlabeled phalloidin (Fig. 1 *f*). This result demonstrated that the fluorescent-conjugated phalloidin binds specifically to the actin filaments within the prehair.

As independent confirmation of the presence of actin in the early prehairs, we stained the tissues with an anti-actin mAb (Amersham Corp.). Again the prehairs stained (Fig. 1 *g*, but the staining was more diffuse, probably due to a lower signal to noise ratio as compared to rhodamine-phalloidin staining), confirming the presence of actin in the early prehairs.

We next used rhodamine-phalloidin staining to study the earliest events in prehair development. F-actin staining of early pupal wings revealed that wing cells were polygonal (often hexagonal) in shape near the apical surface of the epithelium (Fig. 1 *a*), and differed in size across the wing. Smaller cells were found proximally and along the wing veins; larger cells were found distally and near the wing margin (data not shown; see Fig. 3 *a* for the orientation of a pupal wing). Before the first sign of prehair differentiation, bundles of F-actin were found outlining the cell periphery, with the vertices often staining more brightly (Fig. 1 *a*). At the onset of prehair differentiation, the pattern of even bright staining seen at all cell vertices was replaced by a pattern of increased F-actin staining at the distal vertex of each cell (Fig. 1 *b*). A large bundle of actin filaments formed at this vertex, and the extension of this bundle distally was coincident with prehair growth (Fig. 1 *c*). The large bundles of actin filaments filled the prehairs, which pointed distally at all stages studied.

Our EM studies on pupal wings of prehair initiation (Fig. 2 *a*) agreed with our findings by F-actin staining and confirmed the results of Mitchell and co-workers (1983). In the longitudinal EM sections, we found that each prehair initiated from the distal most edge of the cell, and was closely apposed to its distal neighbor cell (Fig. 2 *a*). During the earliest stages of prehair development, the prehair lay flat on its distal neighbor (EM data not shown, Fig. 1 *c*) (Mitchell et al., 1983). As prehairs grew in length, they rose above the pupal wing surface at an increasingly steep angle to the cell surface (Figs. 1 *e* and 2 *a*). The EM sections showed that the pupal wing cells were rich in mitochondria and RER (Fig. 2, *a* and *b*). Coated vesicles near the plasma membrane and deposits (possibly cuticulin) on the apical cell and prehair surface were frequently observed (data not shown). These cellular structures suggested that the pupal wing epithelium at this stage was active in protein synthesis and secretion, probably for making the adult cuticle. Bundles of fine filaments (most likely F-actin based on our rhodamine-phalloidin staining) were found inside prehairs but did not completely fill the interior of the shaft (Fig. 2 *a'*). Examination of the longitudinal EM sections of pupal wing cells did not help us to identify any special organizing structure present at the distal region of cells that seemed likely to be associated with the filaments of the prehair shaft.

The morphogenesis of prehairs occurred asynchronously across the pupal wing (Fig. 3). Differentiation started at the distal wing margin and spread first posteriorly, then anteriorly along the edge of the wing (Fig. 3 *b*). Simultaneously, prehair differentiation spread proximally (Fig. 3, *b* and *c*). There was not a wave front of differentiation (i.e., a visible morphogenetic furrow) as is seen in the eye disc (Ready et al., 1976). Instead, patches of cells appeared to differentiate synchronously. Because the process is asynchronous across the pupal wing, it is not possible to give developmental times for each stage in prehair morphogenesis. The process is rapid, with the entire pupal wing going from no sign of prehair morphogenesis to elevated prehairs during 36–39 h after white prepupae formation at 25°C or 69–74 h at 18°C.

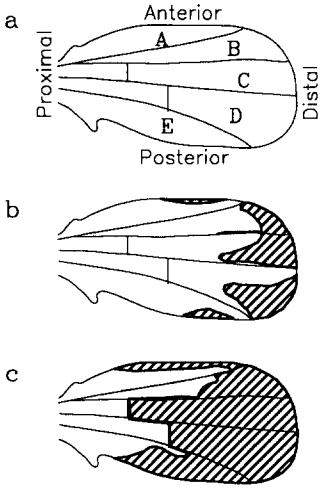

Figure 3. A diagrammatic representation of the asynchrony of prehair differentiation across the pupal wing. (*a*) An early pupal wing before prehair differentiation. The orientation and different regions of the pupal wing are indicated. (*b*) Prehair differentiation starts from the distal region of the wing margin and spreads along the posterior and anterior margin of the wing. Patches of cells with prehairs are found in these regions (*hatched region*). (*c*) At a later time, prehair differentiation has proceeded more proximally and has covered most of the pupal wing. At this stage, one can see shorter prehairs at the proximal region of the pupal wing, and longer prehairs at the distal region of the same wing.

Single Mutant Analysis

We examined mutant phenotypes from six tissue polarity mutations: *fz*, *dsh*, *pk*, *in*, *fy*, and *mwh*. Where possible, the alleles used were phenotypically null or close to null (see Materials and Methods). Since we have a wide range of strong to weak *fz* alleles, we have done a more extensive analysis on this gene than the rest. Besides the hair polarity phenotype, all these mutations cause at least some wing cells to form more than a single hair. In *fz*, *dsh*, and *pk* mutants, only a few cells produce double hairs. In *in* and *fy* mutants, many cells (but not all) form two or three hairs. In *mwh* mutants essentially all cells elaborate more than a single hair. For our single mutant analysis, we examined three phenotypes for each mutation: (*a*) adult wing hair polarity pattern, (*b*) the average number of hairs per cell, and (*c*) prehair initiation site revealed by rhodamine-phalloidin staining. We found that these mutations fell into three phenotypic groups. Group 1 consists of *fz*, *dsh*, and *pk*; group 2 consists of *in* and *fy*; group 3 consists of *mwh*.

Adult Wing Phenotype

Different regions of the adult mutant wings are affected differently by tissue polarity mutations (Figs. 4 and 5; Gubb and Garcia-Bellido, 1982). The wing hair polarity patterns from individuals carrying the same mutation showed minor variations (Adler et al., 1987), but each genotype resulted in a recognizable pattern of polarity disruption. In Fig. 4, we see how hair polarity patterns differ in a small region in the middle of the C region among individual single mutants (Fig. 4, *e*, *i*, *m*, *b*, *c*, and *d*). None of them shows a wild-type polarity pattern (Fig. 4 *a*). In this region, *fz*, *dsh*, and *pk* each shows a characteristic pattern, whereas *in* and *fy* share a similar polarity pattern. It is also clear that *fz*, *dsh*, and *pk* wings contain mostly single hair cells; *in* and *fy* wings contain many double hair cells, and *mwh* wings contain mostly

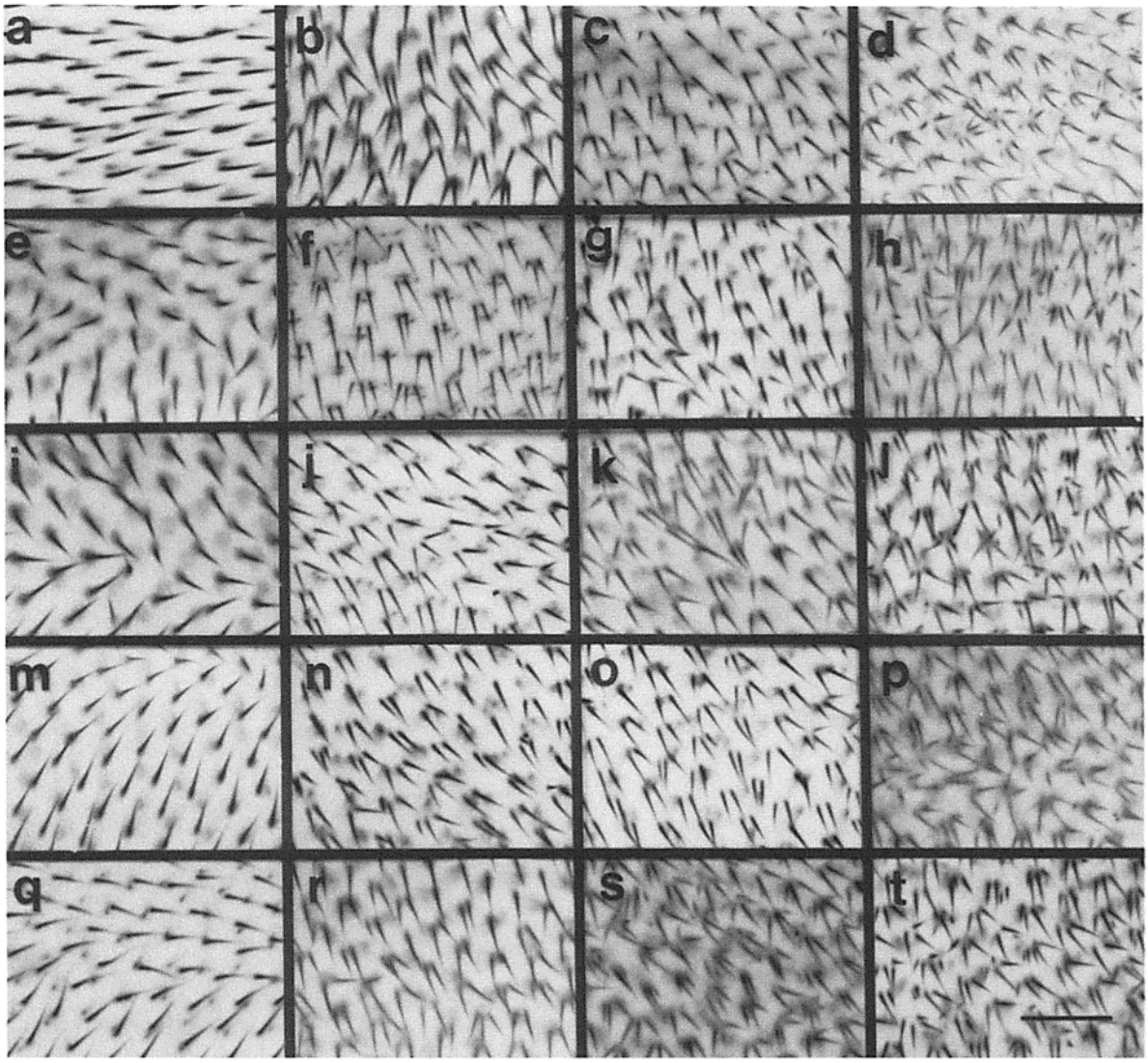

Figure 4. Light micrographs of a small region of adult wings from single and double tissue polarity mutants. Individual micrographs were taken from the dorsal surface and they showed the C region which is just anterior to the posterior cross vein (i.e., near the mid C region). Orientation is the same as in Fig. 3 *a*. (*a*) wild type. *e*, *i*, and *m* are single mutants of the group 1 genes: *fz*, *dsh*, and *pk*, respectively. *b* and *c* are group 2 single mutants of *in*, *fy*, respectively. *d* is a group 3 mutant, *mwh*. *q* is a double mutant of group 1 genes: *dsh; pk*, this double mutant shows mostly single hair cells (compare to *e*, *i*, or *m*). (*f*, *j*, and *n*) Double mutants of group 1 genes and the group 2 gene *in*: *fz in*, *dsh; in*, and *pk; in*, respectively. All of these double mutant combinations had a group 2 mutant phenotype (compare with *b* versus *e*, *i*, or *m*). (*g*, *k*, and *o*) Double mutants of group 1 genes and the group 2 gene *fy*: *fy; fz*, *dsh; fy*, and *fy pk*, respectively. All of these double mutants had a group 2 mutant phenotype (compare with *c* versus *e*, *i*, or *m*). (*h*, *l*, and *p*) Double mutants of group 1 genes and the group 3 gene *mwh*: *mwh fz*, *dsh*; *mwh*, and *pk*; *mwh*, respectively. The double mutant phenotypes resembled *mwh* alone (compare to *d* with *e*, *i*, and *m*). *r*, *fy*; *in* double mutant. This double mutant combination of two group 2 genes resembled both of the individual group 2 mutants (compare with *b* and *c*). (*s* and *t*) Double mutants of group 2 genes with the group 3 gene *mwh*: *mwh in* and *fy; mwh*, respectively. Double mutant phenotypes resembled *mwh* alone (compare with *d* versus *b* and *c*). Bar, 43 μm.

four-or-more-hair cells. The *mwh* cells appear to contain two distinct types of hairs. Some are reasonably long and we refer to these as primary hairs. If we consider only these hairs, the *mwh* cells resemble those seen in *in* and *fy* wings. The *mwh* cells also typically contain several quite small hairs and we call these secondary hairs. These secondary hairs in *mwh* cells separate the *mwh* phenotype from the *in* and *fy* phenotype.

Polarity Pattern. To compare systematically the adult wing patterns, we have simplified the adult wing patterns as shown in Fig. 5 (see Materials and Methods for a detailed description of the simplification scheme). Briefly, the five stripes represent the five regions of the adult wing. Blank regions represent wild-type hair polarity. Regions with arrows represent abnormal patches where the majority (>60%) of hairs point in the indicated direction. Grey regions represent two types of patterns: (*a*) abnormal foci where neighboring hairs do not align (e.g,. Figs. 4 *e* and 7 *f*), or (*b*) more than two APs within a subdivision (e.g., Fig. 4 *q*). We found that two pairs of mutants, *fz* and *dsh*, and *in*

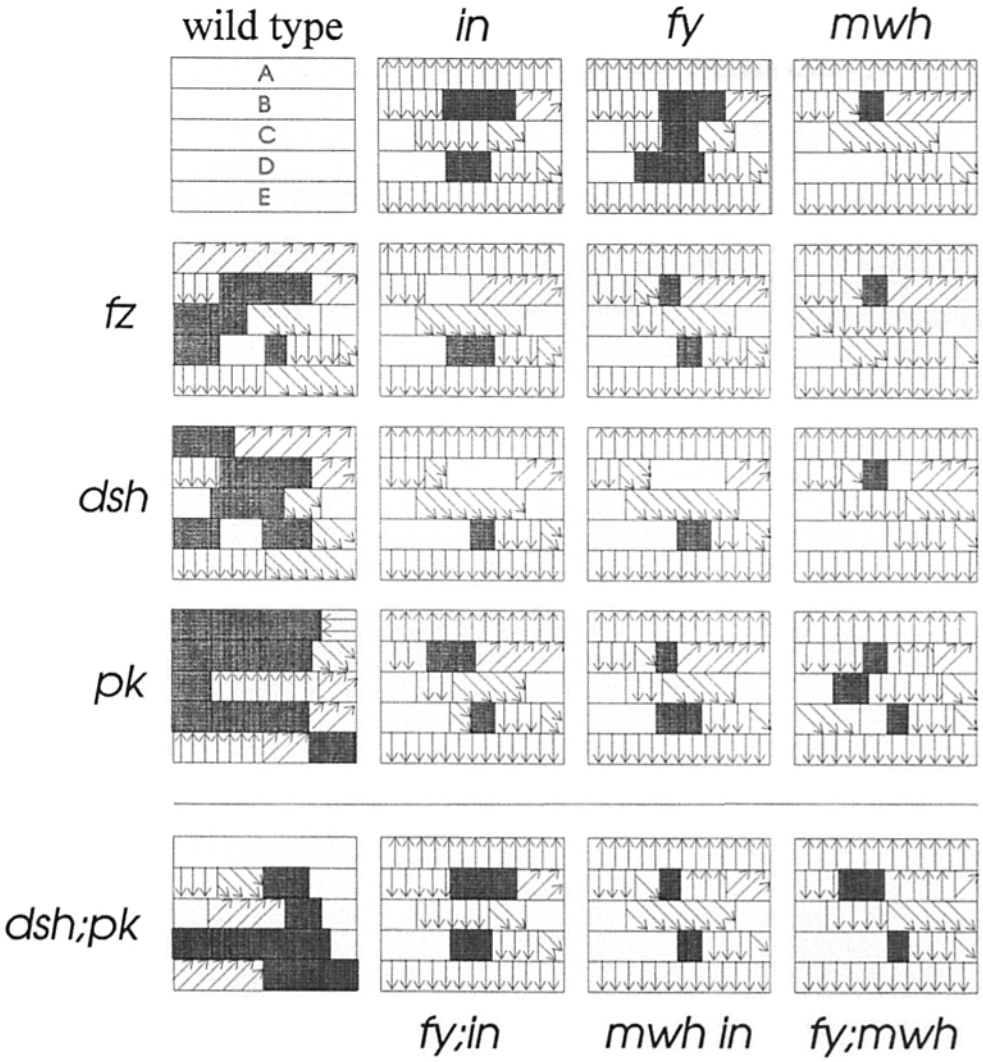

Figure 5. Schematic diagrams of the adult wing hair patterns of single and double tissue polarity mutants. *A–E* indicate the five regions of an adult wing. Orientation is the same as in Fig. 3. Blank regions represent wild-type hair polarity, that is, distally pointing hairs. Regions with arrows represent abnormal patches. The arrows within a subdivision indicate that the polarity of that region is shared by 60% or more of the hairs. Grey regions represent abnormal foci or regions with two or more abnormal patches. The arrangement of the genotypes is the same as in Fig. 4. The polarity patterns of double mutants of group 1 genes (*fz*, *dsh*, and *pk*) and group 2 genes (*in* and *fy*) were similar to the respective group 2 mutants. Similarly, the polarity patterns of group 1 and group 3 double mutants resembled the group 3 mutant. The polarity patterns of group 2 and group 3 double mutants were less disrupted than the group 2 mutants and were similar to the group 3 mutant.

Average Number of Hairs per Cell

	fz	*dsh*	*pk*	*in*	*fy*	*mwh*
fz	1.022 (0.007)	1.010 (0.004)	1.016 (0.006)	1.758 (0.025)	1.966 (0.026)	3.314 (0.035)
dsh		1.014 (0.005)	1.006 (0.004)	1.692 (0.026)	1.734 (0.028)	3.908 (0.040)
pk			1.004 (0.003)	1.902 (0.031)	1.934 (0.026)	3.910 (0.039)
in				1.826 (0.028)	1.912 (0.027)	3.842 (0.028)
fy					1.920 (0.027)	3.394 (0.040)
mwh						3.944 (0.039)

Figure 6. The average number of hairs per cell phenotype for single and double tissue polarity mutants. We counted 100 cells (5 × 20 cells) on the dorsal surface of the C region (similar to the region described in Fig. 4). The number is the mean value of five wings. The SEM (standard deviation divided by the square root of the total number of cells counted) is included within the parenthesis. Means that differ by more than 2 SEM are likely to be different. Group 1 double mutants did not show any changes in the average number of hairs per cell when compared to their respective single mutants. Group 1 and group 2 double mutants became more like group 2 mutants. The group 2 double mutant remained similar to a group 2 single mutant. Group 1 and group 3, group 2 and group 3 double mutants became more like the group 3 single mutant.

and *fy*, shared similar polarity patterns. From these diagrams, we see that the polarity patterns of the group 1 genes (*pk*, *fz*, and *dsh*) are the most abnormal, followed by *in* and *fy*. We did not observe any large AF in a *mwh* wing. In wings carrying weak or moderate *fz* alleles, there were fewer and smaller AFs and APs. In such wings the polarity abnormalities were largely restricted to the proximal and/or central region of the wing.

Average Number of Hairs per Cell. We found three distinct phenotypes for the average number of hairs per cell (Fig. 6). The group 1 mutations *fz*, *dsh*, and *pk* had an average of only marginally more than a single hair per cell (also see Fig. 7*f*). Indeed, >97% of the cells in these wings produced a single hair. For the group 2 mutations *in* and *fy*, an

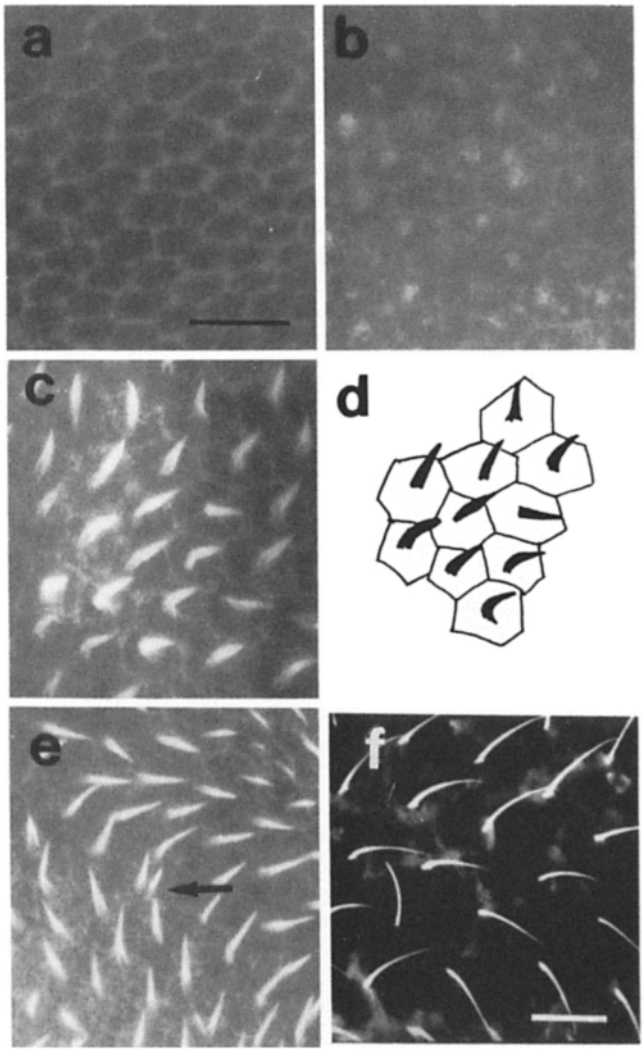

Figure 7. Prehair development of strong *fz* mutants examined by rhodamine–phalloidin staining. (*a*) Pupal wing cells before prehair differentiation. They were hexagonally shaped and were indistinguishable from the wild-type cells (compare with Fig. 1 *a*). (*b*) At the onset of prehair differentiation, F-actin staining was seen near the center of each cell. (*c*) The elongating prehairs were filled with F-actin and had non-distal polarities. (*d*) An interpretive drawing of *c*. Prehairs initiated from cell centers had nondistal polarities. (*e*) A later pupal wing showing an abnormal prehair pattern. A cell that is forming two prehairs is visible and is marked by an arrow. (*f*) A scanning electron micrograph of a strong *fz* mutant adult wing showing an abnormal focus.

average of almost two hairs per cell was found (see also Fig. 9 *d*). The group 3 mutation *mwh* had an average of almost four hairs per cell (see also Fig. 9 *h*).

Pupal Wing Phenotype

We used F-actin staining to examine the early stages in prehair development in mutants. We found that all tissue polarity mutants altered the prehair initiation site. We saw two distinct phenotypes. Pupal wing cells from *fz*, *dsh*, and *pk* had their prehair initiation moved to near the cell center. *in*, *fy*, and *mwh* cells had their prehair initiation along the cell periphery, but not restricted to the distal vertex.

fz. We found that the range of individual cell staining patterns was the same for strong and weak *fz* alleles. Before the onset of prehair differentiation, the cell staining pattern of *fz* pupal wings was indistinguishable from wild type (Fig. 7 *a*). In regions where future APs and AFs formed, we did not see increased staining at the distal vertices. Rather, increased staining was seen near the central region of cells away from the cell periphery (Fig. 7 *b*). The large bundle of actin filaments formed here (Fig. 7, *c* and *d*), and even at the earliest stages, the prehairs did not have a distal polarity (Fig. 7, *c–e*). In longitudinal EM sections of *fz* pupal wings (Fig. 2 *b*), we found that a prehair no longer initiated from the distal most edge of the cell and it never lay flat on the pupal wing surface (data not shown). In strong *fz* alleles, most of the pupal wing cells had prehairs initiated in the central regions of cells. In weak alleles, regions that had dramatic polarity disruption had prehairs initiated from the center of cells. In regions where hair polarity was only mildly affected, we found that prehair initiation sites were along the cell periphery slightly removed from the distal vertex. On occasions, cells with two prehairs were seen (Fig. 7 *e*). These also formed in the central regions of cells.

dsh. The cellular F-actin staining pattern of pupal wings homozygous for dsh^1 (Fig. 8 *a*) was indistinguishable from those of the strong *fz* alleles (Fig. 8 *c*). That is, the large bundle of actin filaments that filled the prehair was assembled near the cell center and the distal polarity was lost. This phenotype was observed in most of the cells in the wing.

pk. The F-actin staining pattern of *pk* pupal wing cells in AFs (Fig. 8 *b*) was identical to those of *fz* and *dsh* (Fig. 8, *a* and *c*). The large bundle of actin filaments was initiated near the cell center and the polarity was nondistal. In large APs, the large bundle of actin filaments was formed at the vertex on the side of the cell where the adult hair ultimately pointed. For example, hairs that pointed anteriorly in an adult wing (e.g., region E) had prehairs initiated from anterior vertices.

in and fy. The cellular F-actin staining pattern of *in* and *fy* pupal wings was indistinguishable. At early stages, we saw several tiny bundles of F-actin staining usually along one edge of the cell periphery (Fig. 9, *a* and *b*). These tiny bundles then resolved into two (or occasionally one or three) actin filled prehairs located along the cell periphery (Figs. 8 *g* and 9 *c*). The polarity of these prehairs followed the site of initiation (e.g., a prehair initiated at a posterior edge of a cell pointed posteriorly). The polarities of the prehairs within the same cell were usually at a small angle (<45°) to one another (Fig. 9 *c*). We have not seen any examples of actin bundles formed in the center of *in* or *fy* cells.

mwh. Prehairs of *mwh* cells also initiated from the cell periphery (Fig. 9 *e*). We saw one or two large bundles of actin filaments formed at an early time. These probably were the precursors of the primary hairs that we saw in the adult wing (Fig. 9 *h*). At a later stage (Fig. 9 *g*), we saw smaller actin bundles near the primary prehairs. These were likely to be the prehairs that would form the secondary hairs (Fig. 9 *h*). We suggest that because these prehairs formed at later stages, they had less time to grow and therefore ended up being quite short.

Double Mutant Analysis

All the double mutant combinations were analyzed in the manner described for the single mutants. We found that the

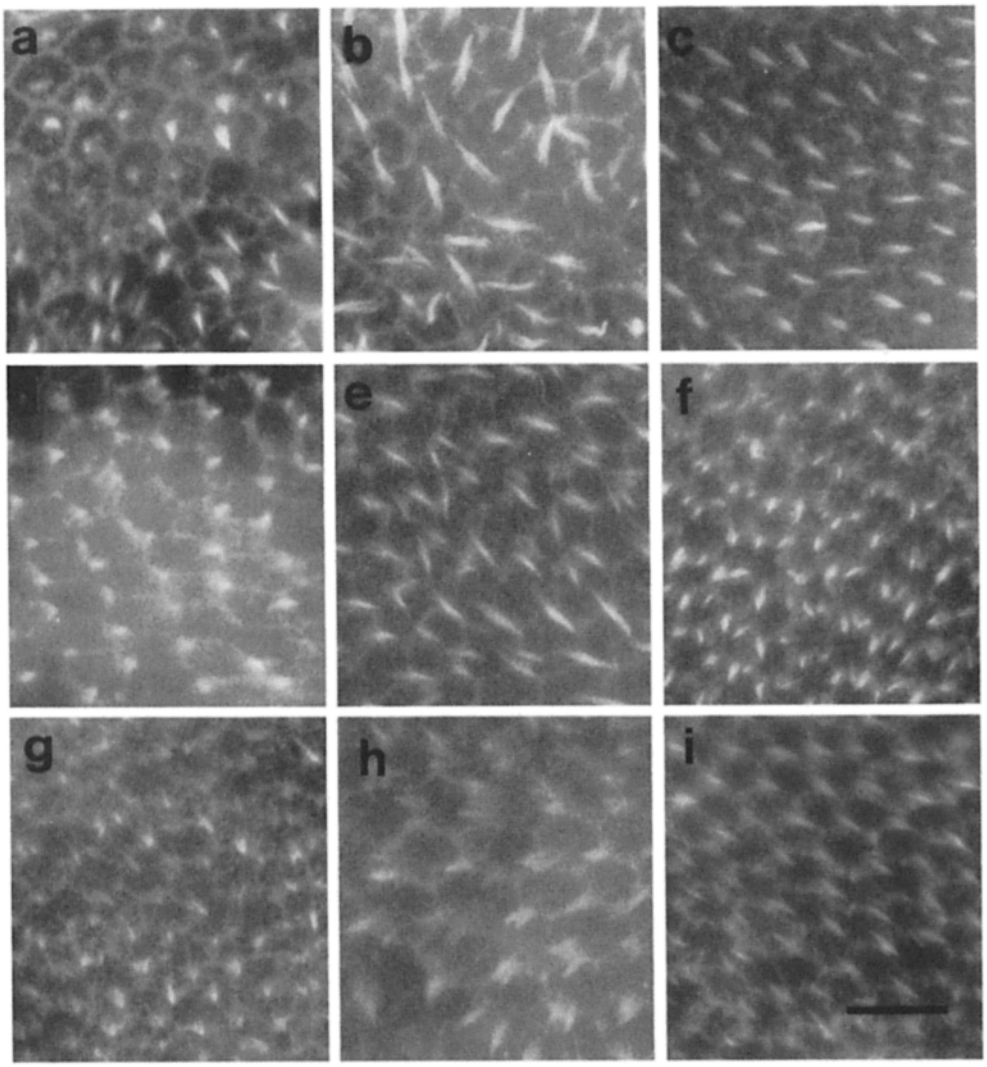

Figure 8. Comparison of the location of prehair initiation site of group 1, group 2, group 3 single mutants with double mutants from between groups. These are rhodamine–phalloidin stained pupal wing cells. Orientation is the same as in Fig. 1. Individual micrographs are from different regions of the pupal wing. *a*, *b*, *c* are *dsh*, *pk*, and *fz*, respectively. These group 1 mutants showed prehair initiation near cell centers. *g* is *in* and it showed prehair initiation along the cell periphery. *d*, *e* are double mutants of *dsh; in*, *pk; in*, respectively. Prehair initiation was along the cell periphery as is seen in the *in* mutant. *i* is *mwh* and prehair initiation was along the cell periphery. *f* is *mwh fz*. It was similar to *mwh* in that prehair initiation was along the cell periphery. *h* is *mwh in* and the prehair initiation was along the cell periphery.

three phenotypic groups described above also represented epistasis groups. Double mutants of group 1 and group 2 mutations resembled group 2 mutants; double mutants of group 1 and group 3 mutations, and group 2 and group 3 mutations resembled the group 3 mutant.

Adult Wing Phenotype

The light micrographs in Fig. 4 show a small region in the middle of the C region for all of the relevant double mutant combinations. Fig. 4, *f*, *i*, and *n* are double mutants between *in* and the group 1 mutations, and Fig. 4, *g*, *k*, and *o* are double mutants between *fy* and the group 1 mutations. We see that these double mutants have many double hair cells resembling *in* and *fy*. The polarity of the double mutants in this region resembles *in* and *fy*. *q* is a double mutant between *dsh* and *pk*. The polarity pattern does not resemble either of the single mutants, and all the cells have single hairs. *r* is a double mutant between *in* and *fy*. The phenotype is similar to the *in* and *fy* single mutants. *h*, *l*, and *p* are double mutants between *mwh* and the group 1 mutations, and *s* and *t* are double mutants between *mwh* and the group 2 mutations. All these double mutants resemble *mwh*.

Polarity Pattern. When we examined the polarity pattern of the whole wing of these double mutants (Fig. 5), we saw a similar trend. All of the double mutants between group 1 and group 2 mutations had polarity patterns that resembled *in* or *fy* (these two single mutants have a similar abnormal polarity pattern). We noticed that the double mutant phenotypes were slightly less disrupted in some regions (e.g., region B). The wing pattern of *fy; in* double mutant resembles *in* or *fy* alone. This result was very different from the group 1/group 1 double mutant between *dsh* and *pk*. The pattern seen in this double mutant resembled neither *dsh* nor *pk* (Fig. 5). The double mutants between group 1 mutations and *mwh* had polarity patterns that were similar to *mwh*, although there was a slight difference in a small region in C. In Fig. 5, the schematic patterns of group 2 and group 3 double mutants showed patterns that were intermediate between the group 2 and 3 single mutants. However, from our direct observations of the double mutant patterns, the greater similarity to the *mwh* pattern was apparent (e.g., lack of any large AF in the group 2 and *mwh* double mutants).

Average Number of Hairs per Cell. Fig. 6 shows the average number of hairs per cell in the dorsal C region for all

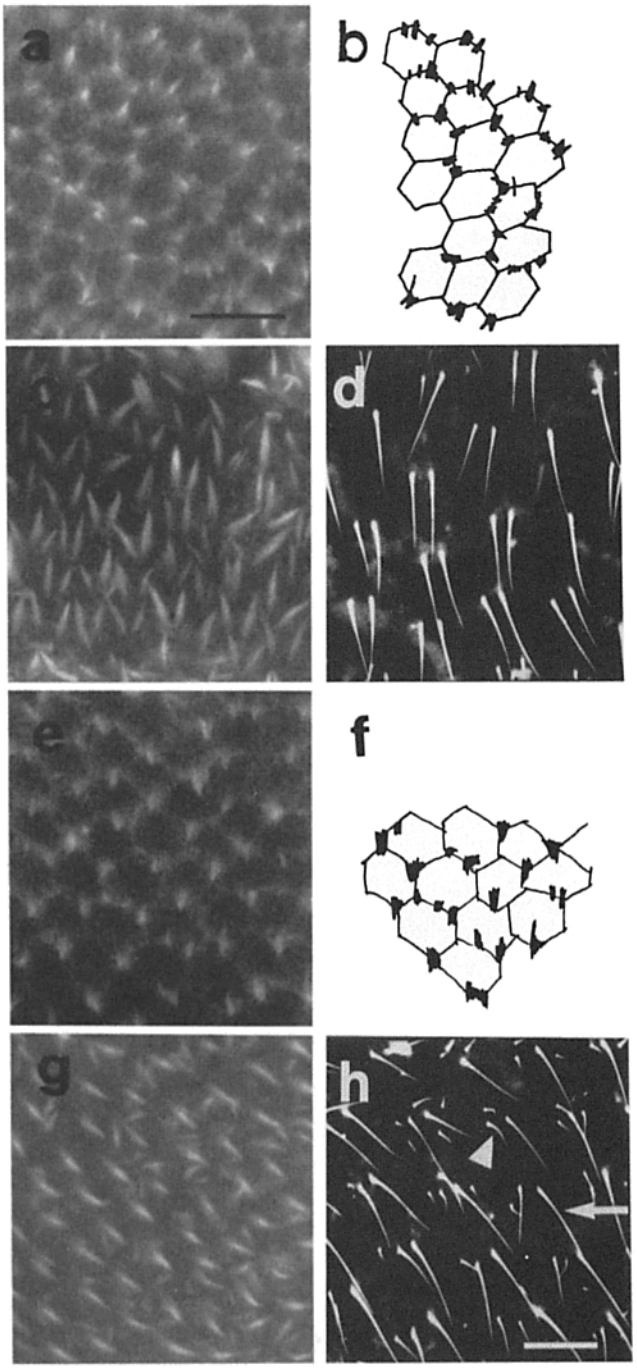

Figure 9. The pupal and adult mutant wing phenotypes of *fy, in* (*a–d*) and *mwh* (*e–h*). (*a*) A *fy* mutant pupal wing during early prehair differentiation showed staining of tiny bundles of F-actin along one side of the cells. An *in* wing looks indistinguishable from the *fy* wing shown in this panel. (*b*) An interpretive drawing of *a*. Note the tiny bundles of F-actin along one side of the cells, the number of prehairs, their initiation sites and polarities. (*c*) A later stage of an *in* pupal wing. The tiny bundles resolved into two (sometimes three) F-actin–filled prehairs of equal size along the same side of the cell periphery. Elongating prehairs had elevated above the pupal wing surface and these prehairs did not point distally. A *fy* wing would be indistinguishable at this stage. (*d*) A scanning electron micrograph of an *in* adult wing. Most cells had two hairs but a few had a single hair. (*e*) An early *mwh* pupal wing showed that most cells had bright F-actin staining at non-distal vertices with some cells had additional bright staining spots along the cell periphery. Prehairs initiated from posterior vertices for most of the cells in this region of the wing. (*f*) An interpretive drawing of *e*. Note that some cells had a single bright staining at the posterior vertex and some had additional bright staining spots along the cell periphery. (*g*) *mwh* pupal wing cells at a later stage showing one or two fairly long prehairs surrounded by several smaller prehairs. Prehairs in this panel had a nondistal polarity. (*h*) A scanning electron micrograph of a *mwh* adult wing. Some cells in this region had two primary hairs (see *arrows*) and some had only one primary hair. All primary hairs were accompanied by a number of secondary hairs (see *arrowhead*).

the double mutant combinations between these six tissue polarity mutations. All double mutants between group 1 mutations essentially had a single hair per cell as was seen for each group 1 single mutant. All of the double mutants between group 1 and group 2 mutations had an average of almost 2 hairs per cell. This is similar to that seen for the group 2 mutants alone. Thus, with respect to this phenotype the group 2 mutations are epistatic to the group 1 mutations. We noticed that the mean values for *dsh; in* and *dsh; fy* were slightly lower than seen for *in* and *fy* single mutants. The significance of this remains to be established. The average number of hairs per cell for the *fy; in* double mutant was similar to the single mutants alone, thus these mutations do not produce an additive effect. Double mutants between *mwh* and any of the group 1 or group 2 mutations had means that ranged from 3.3 to 3.9 hairs per cell. This is similar to that seen for *mwh* single mutants, therefore we conclude that for this phenotype, the *mwh* is epistatic to the group 1 and 2 mutations. Two of the double mutants (*mwh fz* and *fy; mwh*) did show slightly fewer hairs per cell than the *mwh* single mutant.

Pupal Wing Phenotype. We examined all of the double mutant combinations by F-actin staining of pupal wings. Examples of their phenotypes are shown in Fig. 8. Double mutants between group 1 and group 2 mutations (Fig. 8, *d* and *e*) resembled group 2 mutants (*g*). In most cells, two actin bundles formed at nondistal vertex locations along the cell periphery. Double mutants between group 1 and group 3 (Fig. 8 *f*) mutations resembled the group 3 mutant. Multiple actin bundles formed at the cell periphery. Double mutants between group 2 and group 3 mutations (Fig. 8 *h*) resembled a *mwh* (group 3) mutant. We saw one to three actin bundles formed at the cell periphery, and additional small bundles were seen at later stages, as they were observed in a *mwh* mutant. The prehair initiation phenotype revealed the same epistatic relationships among group 1, 2, and 3 mutants as we had observed in adult wing patterns and the average number of hairs per cell phenotypes.

Discussion

F-actin Is Abundant in Prehairs

We have found that *Drosophila* prehairs are filled with large bundles of actin filaments. We have used this property of prehairs to study early events in prehair development. We suggest that directed F-actin polymerization at the distal vertex may be the driving force for plasma membrane extension, and thus prehair formation. The phenomenon of actin polymerization in prehair initiation may be similar to the

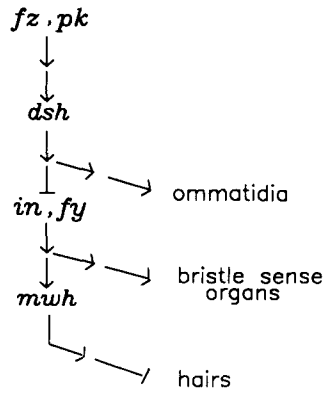

Figure 10. A model of the tissue polarity pathway in the regulation of hair polarity in the *Drosophila* wing. Group 1 mutations affect the orientation of all three structures: ommatidia, bristles, and hairs. Group 2 mutations affect bristles and hairs. The group 3 mutation affects hairs only.

acrosomal reaction in activated echinoderm sperms (Tilney et al., 1973). Tissue polarity genes may control the choice of the prehair initiation site by regulating F-actin assembly in a pupal wing cell. It seems likely that actin binding proteins (for a review see Hartwig and Kwiatkowski, 1991) will play a role in the regulation of prehair initiation and hair polarity. The distribution or localized activation (or inactivation) of certain actin binding proteins may dictate the site for F-actin assembly and attachment to the cell membrane, thus establishing the polarity of the adult hair. We speculate that actin binding proteins may be the final regulatory targets of the tissue polarity genes.

Prehairs appear at least superficially similar to the microvilli found on many vertebrate intestinal epithelial cells both in general appearance and by the presence of a large bundle of actin filaments. Prehairs differ from the microvilli in that F-actin bundles do not fill the prehairs completely, and the base of prehair lacks a major F-actin meshwork as is seen in the organized terminal web of microvilli. Whether these two cellular structures are truly homologous and whether they share molecular constituents other than F-actin remains to be established.

Asynchrony of Prehair Differentiation

Prehairs differentiate in patches, starting at the distal wing margin and spreading proximally and interiorly. This asynchrony in prehair differentiation is not unique. In the milkweed bug, Lawrence (1966) observed asynchronous differentiation of hairs and bristles. He speculated that this asynchronous differentiation might reflect asynchronous determination of new hair and bristle centers. In the *Drosophila* pupal wing, we doubt that this is the case since almost all wing cells produce a prehair.

Cell Geometry and Constant Prehair Initiation Site Confer the Regular Spacing of Adult Wing Hairs

There is a very strong correspondence between the actin staining pattern in the pupal wing and the wing hair pattern in the adult for both wild-type and mutant flies. There is only a difference in the size of the hairs and cells at these stages (see Fig. 1, *a* and *f* for size differences). This indicates that the hair polarity pattern seen in the adult wing is the final product of the earlier events that we observe via F-actin staining. Thus, it should be possible to understand how the adult wing pattern is generated by studying the F-actin pattern of pupal wing cells.

On the adult wing, hairs are evenly spaced and are found in rows. This appears to be a consequence of the hexagonal cell shape, the regular packing of the pupal wing cells, and the use of a common subcellular location (distal vertex) within these cells for the assembly of the actin bundle that forms the prehair. In this respect the *Drosophila* wing follows a common strategy of biological systems in using the regular packing of subunits to build a large structure with repeated properties. The *Drosophila* wing falls between a virion and a honeycomb in scale.

Hair Polarity Is Regulated by Tissue Polarity Genes at the Initiation of Prehair Formation

Hair polarity appears to be regulated at an early stage in hair development, presumably prehair initiation, as from the earliest stage that we can detect prehairs they have a distal orientation. We suggest that hair polarity is controlled by the tissue polarity genes regulating the subcellular location for prehair initiation. There are several pieces of data that support this hypothesis. One is that all wild-type cells use the distal vertex for prehair initiation and the resulting hairs all have a distal polarity (Fig. 1). Furthermore, all mutations that alter prehair polarity also alter the subcellular location for prehair initiation. For example, in *fz* mutant wings, prehairs no longer initiate from the distal vertex, instead, they initiate randomly in the central region of the cells (Fig. 7). Simultaneously, the polarity of these hairs becomes grossly abnormal. Mutations in the group 2 and 3 genes, which produce less dramatic effects on adult wing hair polarity than the group 1 genes result in prehair initiation at peripheral locations other than the distal vertex (Fig. 9). Further evidence of the tight coupling of prehair initiation site and hair polarity comes from the E region of *pk* mutant wings where hairs that point anteriorly have prehairs that initiate from the anterior vertices of cells. This tight coupling is also seen in regions of *in*, *fy*, and *mwh* mutant wings (e.g., regions A and E).

We have no data on a possible mechanism by which the location for prehair initiation determines the direction of prehair growth. The observation that a prehair does not form perpendicularly to the cell surface, but lies flat on its distal neighbor cell early in development argues for a cell–cell contact or ligand–receptor type interaction as a possible mechanism for the distal growth of prehairs. Alternatively, interactions between the F-actin bundle in the prehair and the cortical actin filaments could be providing orientation guidance.

The observation that mutations in all six of the tissue polarity genes studied resulted in at least some cells forming more than one hair is also consistent with these genes functioning to regulate prehair initiation. The high frequency of multiple-hair cells in mutants for group 2 and 3 genes (Fig. 6) suggests to us that these genes function closer to the prehair initiation step than the group 1 genes. They can be thought of as encoding proteins that function as inhibitors of prehair initiation. The low frequency of multiple-hair cells in group 1 mutants suggests that these genes only indirectly regulate prehair initiation. This is consistent with previous results that suggested that an abnormal intercellular polarity signal distal to a mitotic clone of *fz* mutant cells could induce genetically wild-type wing cells to form more than one hair

(Vinson and Adler, 1987). One possible function of the group 1 genes is to inhibit locally the activity of group 2 and 3 genes to allow prehair initiation at the distal vertex (see Fig. 10 and below for a detailed discussion of this model).

Tissue Polarity Mutations Fall into Three Phenotypic and Epistasis Groups

Examination of the adult and pupal wing phenotypes of the six tissue polarity mutations led us to conclude that these mutations fall into three phenotypic groups. The three group 1 mutations: *fz*, *dsh*, and *pk* result in most wing cells forming a single hair that is derived from a prehair initiated near the cell center. The similarity of the *fz* and *dsh* phenotypes suggest that these two genes have a closely related function. The group 2 mutations *in* and *fy* have a similar phenotype and therefore we suggest that they also may have a closely related function. The significance of the phenotypic groupings is supported by our finding that these groups are also epistasis groups. This leads us to suggest that the three groups of genes are affecting different parts of a regulatory pathway that restricts prehair initiation to the distal vertex of pupal wing cells. There are several reasons that we argue for a regulatory pathway. To a first approximation, all these mutations affect the orientation but not the morphology of the cuticular structures. Further, the group 1 mutations affect ommatidia, bristle sense organs and hairs. These cuticular structures are morphologically quite distinct. Thus, we think it unlikely that the tissue polarity genes encode major structural components shared by these different types of cuticular structures. Moreover, mutations in two of the group 1 genes (*fz* and *pk*) are non-cell autonomous in genetic mosaics (Gubb and Garcia-Bellido, 1982; Vinson and Adler, 1987). This shows that these genes are required for intercellular signaling, which is more likely to be regulatory than structural in nature. We propose that the group 1 genes (*fz*, *dsh*, and *pk*) are upstream of the two group 2 genes (*in* and *fy*), which are in turn upstream of the group 3 gene *mwh* (Fig. 10).

Possible Functions of Tissue Polarity Genes

In genetic mosaics, *pk* mutations and most *fz* alleles (including null alleles) are non-cell autonomous, arguing that both genes are essential for the generation or transmission of an intercellular polarity signal (Gubb and Garcia-Bellido, 1982; Vinson and Adler, 1987). In the case of *fz*, the non-cell autonomy appears directional, suggesting that the signal is transmitted along the proximal–distal axis of the wing (Vinson and Adler, 1987). A second class of *fz* alleles are cell autonomous, suggesting that *fz* is also required for the transduction of the intercellular signal (Vinson and Adler, 1987) to the actin cytoskeleton. The deduced sequence of the Fz protein suggests that it encodes a protein with seven putative transmembrane domains (Vinson et al., 1990). Indeed, recent experiments have shown that the Fz protein is a cell surface protein with an odd number of transmembrane domains (Park, W. J., J. Liu, and P. N. Adler, manuscript submitted for publication). The structure of the Fz protein suggests that it could be a cell surface receptor, although receptors are not normally expected to be non-cell autonomous. A possibility is that *fz* is analogous to the cAMP receptor for cellular aggregation in *Dictyostelium* (Johnson et al., 1989), and that it is a receptor that uses two distinct signal transduction pathways. One of these pathways would lead to the relaying of the signal to its neighboring cells, and the other to restricting prehair initiation to the distal vertex. Mutations in *fz* that disrupt both pathways or only disrupt the relaying signal transduction pathway will be non-cell autonomous, while those that only disrupt the pathway that leads to restricting prehair formation to the distal vertex will be cell autonomous (such as the cell autonomous fz^{N21} and fz^{F31} alleles) (Vinson and Adler, 1987). Thus, this model allows us to account easily for a single *fz* protein carrying out both cell autonomous and nonautonomous functions (Krasnow, R., and P. N. Adler, unpublished observation), and suggests possible roles for other group 1 tissue polarity genes.

The *pk* gene also acts non-cell autonomously (Gubb and Garcia-Bellido, 1982). Based on our model for *fz* action, the *pk* gene could either be required for the synthesis of the ligand *fz* binds or it could encode a component of the signal relaying pathway.

The *dsh* gene is involved in both tissue polarity and segment polarity formation. In the early embryo, *dsh* is required to maintain the posterior compartment of each segment. Its maternal effect embryonic lethal phenotype is very similar to the *wingless* (*wg*) phenotype (Perrimon et al., 1987; Klingensmith, J., and N. Perrimon, personal communication). Wingless is a secreted protein that acts as an intercellular signal to establish and maintain the segmental pattern in the embryo (McMahon and Moon, 1989; Klingensmith, J., and N. Perrimon, personal communication). It has been shown that *dsh* acts cell autonomously in both embryonic and imaginal development (Klingensmith, J., and N. Perrimon, personal communication; Marsh, J. L., personal communication), leading to the hypothesis that Dsh is a cellular factor that acts downstream of *wg* and is required for the transduction of the *wg* signal (Klingensmith, J., and N. Perrimon, personal communication). From our study of *dsh* in tissue polarity formation, we suggest that *dsh* has a similar function in the *fz* tissue polarity pathway, and that it is a protein that functions in several signal transduction pathways in the cell.

The multiple-hair cell phenotypes of *in*, *fy*, and *mwh* suggests that these genes act as inhibitors of prehair initiation. These genes seem likely to affect the assembly of the large bundle of actin filaments that forms the prehair by encoding proteins that modulate the activity of actin binding proteins (or by encoding actin binding proteins themselves). The fact that *in* and *fy* mutations affect the polarity of both hairs and bristle sense organs, which are quite different structures, suggests that these genes encode proteins that function in a signal transduction pathway as regulators or modulators of the activity of other cellular proteins. On the other hand, the *mwh* mutation affects hairs only; thus, we speculate that this gene could encode a protein that interacts directly with actin to regulate the formation of the large bundle of F-actin found in the prehair. Tests of these hypotheses will first require the molecular cloning and sequencing of these genes.

The epistasis of the group 2 and 3 genes to the group 1 genes indicates that the function of the group 1 genes is not essential for having prehair initiation being restricted to the cell periphery. Rather, this is the case only when the class 2 and 3 genes are functioning. We suggest that the group 1 genes function to inhibit locally the activity of the group 2 and 3 genes at the distal vertex, and thus lift the inhibition of prehair initiation at this location. In the absence of group

1 gene function prehair initiation is inhibited in all regions and prehair initiation occurs in a spatially relatively random manner along the apical surface of the pupal wing epithelial cells. Prehair initiation at the cell periphery in the absence of group 2 and group 3 gene function may reflect the distribution of a putative unknown activator of prehair initiation.

In a wild-type wing, all cells form a single hair. A variety of models can account for this restriction. For example, prehair initiation could commence at the proper time due to an activator accumulating to a critical threshold concentration (and inhibitors being locally inactivated). One consequence of prehair formation could be the stimulation of degradation of the activator. The secondary hairs that form later in *mwh* wings could be explained in such a model by *mwh* being required for the degradation of the activator.

Evidence for an Additional System Involved in Tissue Polarity

Our data argues that the normal wing hair pattern is regulated by a genetic pathway that restricts prehair initiation to the distal vertex of pupal wing cells. Based on the wild-type wing pattern alone, the use of the distal vertex as the prehair initiation site seems sufficient to explain the wild-type pattern. However, mutant wing patterns reveal the existence of an additional system (Adler et al., 1987). Typically, individual hairs on a mutant wing do not display random polarities. Rather, their polarity is at least somewhat similar to their neighbors. This results in APs when neighbors have essentially the same abnormal polarity (Fig. 9 *d*), and some AFs with distinctive swirls when neighbors differ slightly in orientation (Fig. 7 *f*). This coordination of hairs, prehairs, and the actin cytoskeleton among neighboring cells is still functional in all known tissue polarity mutants, and therefore must have an independent genetic basis. At this stage, we have no data on how this coordination is achieved, but we speculate that the inter-connection of F-actin network (possibly via actin binding proteins) among neighboring cells is a likely candidate for this aspect of tissue polarity formation.

We thank Drs. A. L. Beyer, C. R. Cronmiller, and R. Rodewald for comments on the manuscript. We are indebted to Dr. R. Rodewald for his help in the EM work. We also thank everyone in the Adler lab for a friendly and stimulating working environment.

This work was supported by National Institutes of Health grant GM37136.

Received for publication 2 December 1992 and in revised form 9 July 1993.

References

Adler, P. N. 1992. The genetic control of tissue polarity in *Drosophila*. *BioEssays* 14:735–741.

Adler, P. N., J. Charlton, and C. Vinson. 1987. Allelic variation at the *frizzled* locus of *Drosophila*. *Dev. Genet.* 8:99–119.

Adler, P. N., C. Vinson, W. J. Park, S. Conover, and L. Klein. 1990. Molecular structure of *frizzled*, a *Drosophila* tissue polarity gene. *Genetics.* 126: 401–416.

Bopp, D., L. R. Bell, T. W. Cline, and P. Schedl. 1991. Developmental distribution of female-specific *Sex-lethal* proteins in *Drosophila melanogaster*. *Genes & Dev.* 5:403–415.

Garcia-Bellido, A., and J. R. Merriam. 1971. Parameters of the wing imaginal disc development of *Drosophila melanogaster*. *Dev. Biol.* 24:61–87.

Gubb, D., and A. Garcia-Bellido. 1982. A genetic analysis of the determination of cuticular polarity during development in *Drosophila melanogaster*. *J. Embryol. Exp. Morphol.* 68:37–57.

Hartwig, J. H., and D. J. Kwiatkowski. 1991. Actin-binding proteins. *Curr. Opin. Cell Biol.* 3:87–97.

Held, L. I. Jr., C. M. Duarte, and K. Derakhshanian. 1986. Extra tarsal joints and abnormal cuticular polarities in various mutants of *Drosophila melanogaster*. *Roux's Arch Dev. Biol.* 195:145–157.

Johnson, R. L., R. Gundersen, P. Lilly, G. S. Pitt, M. Pupillo, T. J. Sun, R. A. Vaughan, and P. N. Devreotes. 1989. G-protein-linked signal transduction systems control development in *Dictyostelium*. *Dev. Supp.* 75–80.

Lawrence, P. A. 1966. Development and differentiation of hairs and bristles in the milkweed bug, *Oncopeltus fasciatus* (Lygaeidae, Hemiptera). *J. Cell Sci.* 1:475–498.

Lawrence, P. A. 1973. The development of spatial patterns in the integument of insects. *In* Developmental System: Insects. S. J. Counce and C. H. Waddington, editors. Academic Press, New York. Vol. 2. 157–206.

Lindsley, D. L., and G. G. Zimm. 1992. The Genome of *Drosophila melanogaster*. Academic Press, New York. 1133 pp.

McMahon, A. P., and R. T. Moon. 1989. *int-1* a proto-oncogene involved in cell signalling. *Dev. Supp.* 161–167.

Mitchell, H. K., J. Roach, and N. S. Petersen. 1983. The morphogenesis of cell hairs on *Drosophila* wings. *Dev. Biol.* 95:387–398.

Perrimon, N., and A. P. Mahowald. 1987. Multiple functions of segment polarity genes in *Drosophila*. *Dev. Biol.* 119:587–600.

Ready, D. F., T. E. Hanson, and S. Benzer. 1976. Development of the *Drosophila* retina, a neurocrystalline lattice. *Dev. Biol.* 53:217–240.

Schubiger, M., and J. Palka. 1987. Changing spatial patterns of DNA replication in the developing wing of *Drosophila*. *Dev. Biol.* 123:145–153.

Tilney, L. G., S. Hatano, H. Ishikawa, and M. S. Mooseker. 1973. The polymerization of actin: its role in the generation of the acrosomal process of certain Echinoderm sperm. *J. Cell Biol.* 59:109–126.

Tucker, J. B. 1981. Cytoskeletal coordination and intercellular signalling during metazoan embryogenesis. *J. Embryol. Exp. Morphol.* 65:1–25.

Vinson, C., and P. N. Adler. 1987. Directional non-cell autonomy and the transmission of polarity information by the *frizzled* gene of *Drosophila*. *Nature (Lond.).* 329:549–551.

Vinson, C. R., S. Conover, and P. N. Adler. 1989. A *Drosophila* tissue polarity locus encodes a protein containing seven potential transmembrane domains. *Nature (Lond.).* 338:263–264.

Wulf, E., A. Deboben, F. A. Bautz, H. Faulstich, and Th. Wieland. 1979. Fluorescent phallotoxin, a tool for the visualization of cellular actin. *Proc. Natl. Acad. Sci. USA.* 76:4498–4502.